Hindawi
Journal of Chemistry
Volume 2023, Article ID 9756592, 1 page
https://doi.org/10.1155/2023/9756592

Retraction

Retracted: Electrochemical Mechanical Properties of Beam-Column Joints of Building Steel Structures under Impact Loads

Journal of Chemistry

Received 15 August 2023; Accepted 15 August 2023; Published 16 August 2023

This article has been retracted by Hindawi following an investigation undertaken by the publisher [1]. This investigation has uncovered evidence of one or more of the following indicators of systematic manipulation of the publication process:

(1) Discrepancies in scope
(2) Discrepancies in the description of the research reported
(3) Discrepancies between the availability of data and the research described
(4) Inappropriate citations
(5) Incoherent, meaningless and/or irrelevant content included in the article
(6) Peer-review manipulation

The presence of these indicators undermines our confidence in the integrity of the article's content and we cannot, therefore, vouch for its reliability. Please note that this notice is intended solely to alert readers that the content of this article is unreliable. We have not investigated whether authors were aware of or involved in the systematic manipulation of the publication process.

Wiley and Hindawi regrets that the usual quality checks did not identify these issues before publication and have since put additional measures in place to safeguard research integrity.

We wish to credit our own Research Integrity and Research Publishing teams and anonymous and named external researchers and research integrity experts for contributing to this investigation.

The corresponding author, as the representative of all authors, has been given the opportunity to register their agreement or disagreement to this retraction. We have kept a record of any response received.

References

[1] L. Qian, "Electrochemical Mechanical Properties of Beam-Column Joints of Building Steel Structures under Impact Loads," *Journal of Chemistry*, vol. 2022, Article ID 4942187, 9 pages, 2022.

Hindawi
Journal of Chemistry
Volume 2022, Article ID 4942187, 9 pages
https://doi.org/10.1155/2022/4942187

Research Article

Electrochemical Mechanical Properties of Beam-Column Joints of Building Steel Structures under Impact Loads

Liu Qian

Anhui Vocational and Technical College, Hefei 230062, Anhui, China

Correspondence should be addressed to Liu Qian; 31115302@njau.edu.cn

Received 24 April 2022; Revised 19 May 2022; Accepted 26 May 2022; Published 7 June 2022

Academic Editor: Aruna K K

To optimize the seismic performance in high-rise buildings, the performance changes of beam-column joints of high-rise steel structures of buildings when they are impacted are analyzed to obtain the optimal choice of joint combination. The most commonly used steel beam and steel column joints are selected as the research objects. Firstly, the finite element model and the shell element model of the force are established and then the model of the finite element combination of six kinds of steel beam and steel column joints is established. Secondly, the applied data of common impact force in actual buildings are collected, and the simulated impact force in this experiment is established according to the sampled data. Then, the changes in each performance of the joints under the action of the impact external force are deeply explored through simulation. Finally, the accuracy of the model is confirmed by calculation. The experimental results comprehensively show that the transmission mechanisms of the impact force are different for the six joints. Through calculation and comparison, the bending stiffness, strength, deformation, the displacement degree of the joints, and the bearing degree of the impact external force are comprehensively analyzed. It is concluded that the bolt-type and external diaphragm-type steel tube column concrete and steel-beam concrete composite joints have better seismic resistance than the other five joints. The bolt-type does not need to be welded on site, and the on-site construction workers only need to assemble, which can reduce the technical requirements for construction workers, improving the practicability and applicability. Therefore, it shows reliable reference significance for the joint selection of building steel structures.

1. Introduction

Steel structures are widely used in buildings [1]. When subjected to other external forces, steel structures can withstand very good compressive bearing capacity because steel has strong toughness and plasticity. Steel usually appears in the form of construction or formwork in construction, which can effectively save the time and manpower and material resources of repeated disassembly and assembly of formwork on the construction site and improve the construction efficiency. Because the general steel is very thin, it is often easy to process and reuse, which saves a lot of construction costs. The research results of many architectural scholars have shown that steel structure is the preferred material, with light weight and good seismic performance. In recent years, steel structures have become the mainstream materials in the construction field [2] and are often used as important building structures such as beam-column joints.

Many scholars in the world have simulated in-depth experimental research on beam-column joints of steel structures through a large number of experimental data and theoretical analysis and analyzed and summarized the relevant calculation theories, design methods, and calculation equations of steel structures. With the application and expansion of the theory in engineering, the relevant specifications and recommended standards for steel have been promulgated [3], and the steel structure technology has been listed as one of China's scientific and technological achievements. In addition, the calculation equation of the joint's bearing limit was also deduced; the beam-column joint type with better seismic performance was studied through the experimental mechanism. Some researchers have conducted experiments on compressive, flexural, and impact bearing capacity for different types of beam-column joints [4] and simulated and analyzed them and obtained calculation formulas that can be extended to actual construction projects.

As the performance of building steel structures is gradually excavated and tested, there is a choice of welding materials for joints on the combined modules of steel structures. At present, there is no more accurate optimal solution because there is no comprehensive conclusion on the stability, seismic resistance, and impact resistance of building beams or building column joints. Therefore, the cross-shaped member of the concrete-filled steel tube (CFST) beam and column is undertaken as an example in this work to establish the experimental basis and carry out the finite element calculation. Firstly, separate experiments are carried out on CFST beams and CFST columns [5] to study their endurance and resistance under load. Secondly, the bearing force, stress distribution, energy consumption, the curve state of the connecting skeleton, and the degree of degradation and damage are analyzed. Finally, the impact resistance advantages and disadvantages of each combination module are obtained through various experimental studies. In addition, the applicable environment of the steel structure joint module is summarized, which provides an important technical support for the selection of the steel structure beam-column joint combination mode. Results here can provide reference significance for the selection of joints of building steel structures.

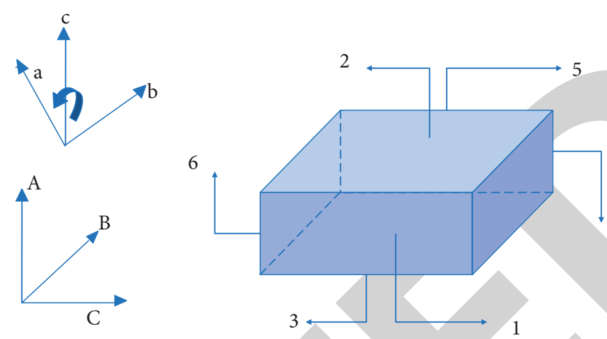

Figure 1: The steel pipe unit model.

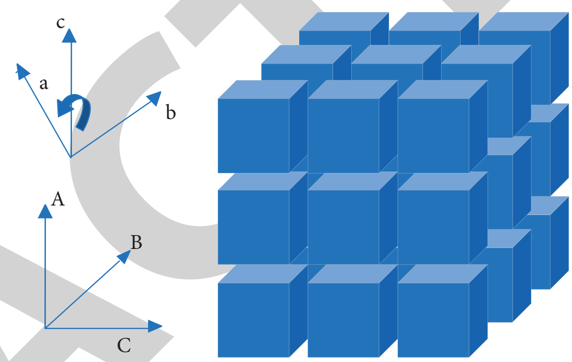

Figure 2: The C3D8R unit model.

2. Mechanical Properties of the Impact Load Based on CFST Beam-Column Joints

2.1. Establishment of the Force Finite Element Model for Beam-Column Joints. Four joint-reduced general shell element models are used to construct the steel pipe element model [6]. The selection of this kind of the shell element model can facilitate us to solve the problem through two theories of thin shell and thick shell in the experiment. It also has good plasticity and elasticity. For simulation experiments, it has been able to extremely realistically restore the deformation and stress of the steel pipe under pressure during specific construction. After the steel pipe element model is selected, it is necessary to add a baffle plate with a baffle plate and the material adopts the element model of eight joint reductions. The baffle is added at the end of the steel column or steel beam to provide a carrier for the impact force in the later experiment. This element model will have a slight distortion of the mesh, but it does not affect the experimental results and still meets the error range. The model of the CFST is constructed by the C3D8R element of the Open System for Earthquake Engineering Simulation (OpenSEES) software [7]. The advantage of this unit is that it can realistically simulate the state and the working state of the improved performance of concrete under the mixing of steel tubes. The steel pipe unit model and the C3D8R unit model are shown in Figure 1 and 2, respectively.

Each joint in the steel pipe element model contains 6 dimensions, including the direction of movement along the A, B, and C axes in the plane and the direction of rotation around the A, B, and C axes. The 6 joints are, respectively, represented in the figure, which can accurately and clearly show the change in the mechanical properties of the steel pipe under the impact force. The eight joint three-dimensional solid model of the baffle and the concrete-filled steel tubular element model are both based on the C3D8R element model, which can effectively reduce the degree of freedom and improve the efficiency [8]. The obtained data can be more accurate, each joint also has 6 dimensions, which is the same as the dimension direction of the steel pipe unit model. The element is capable of simulating nonlinear materials and can clearly study their elastic and plastic deformation and damage.

For the finite element joint model established in this work, there are six types of simulation combinations, as shown in Figure 3.

The figure shows the joint forms of the three column top shafts under pressure and the load and the sequential combined model diagram of the two connection methods. The three joints are steel tube column and steel beam, CFST column and steel beam, and CFST column and CFST beam. The two connection methods are the bolt-type and the external diaphragm-type [9].

2.2. Parameter Selection and Simulation Calculation of the Finite Element of Each Test Piece. The ingredients of concrete in this simulation experiment are water, cement, fine sand, crushed stone, and water reducer, and the ratio is 1 : 2.4 : 3.4 : 4.1 : 0.0005. The parameters of the selected steel pipe are the

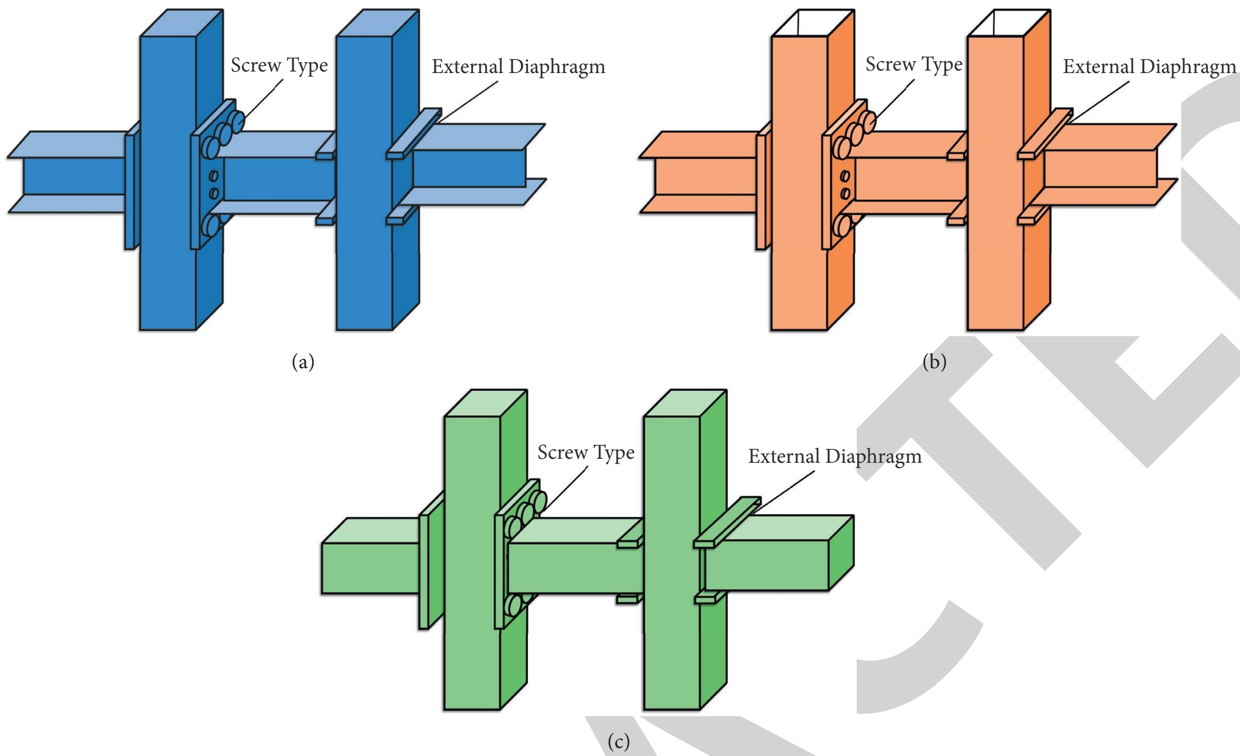

Figure 3: Model diagrams of six types of simulated combination modes: (a) steel tube column and steel beams; (b) CFST columns and steel beams; (c) CFST columns and steel-tube-beam.

wall thickness of 6 mm and the perimeter of the section of the pipe string of 250 mm. After the predetermined value is set, the calculation is carried out according to the relevant regulations, the material of the steel pipe in practical application and the strength of the concrete prepared in this experiment. The calculation equation of the bearing pressure value of the pipe string is given as follows:

$$N_{\rho} = f_{s} A_{s}. \qquad (1)$$

In the above equation, N_ρ is the bearing pressure value of the pipe string, f_s is the yield strength of the pipe, and A_s represents the variance value of the pipe string. When the beam-column joint is subjected to an impact force, in addition to the displacement deformation, there is also the deformation amount at yielding that needs to be considered [10]. For the convenience of research, the analysis and calculation of displacement ductility is set up in this paper, that is; the ratio between the deformation degree and the yield deformation is calculated by the equation. If the ductility is large, it means that the impact resistance is good; otherwise, it means that the resistance is not good. The equation for the calculation of the displacement ductility is expressed as follows:

$$m = \frac{\Delta x}{\Delta y}. \qquad (2)$$

The difference in x is the deformation, the difference in y is the deformation at yield, and m is the displacement ductility.

The calculation equations for the bending stiffness value of the cross section of the steel tube column and the bending stiffness value of the steel beam are the same, expressed as follows:

$$EI = E_{s} I_{s}. \qquad (3)$$

In aforementioned equation (3), EI is the bending stiffness of the CFST column, E_s is the elastic modulus, and I_s refers to one-twelfth of the side length of the steel tube column to the fourth power.

The equation for calculating the bending bearing capacity of the beam is as follows:

$$M_{uk} = \left[0.5 A_{s}\left(h - 2t - d_{n}\right) + bt\left(t + d_{n}\right)\right] f_{y}. \qquad (4)$$

In equation (4), A_s is the longitudinal reinforcement area, h is the beam height, b is the beam width, and f_y is the flexural strength.

The calculation results of each index of the bearing pressure value of the pipe string, the bending stiffness value of the cross section, the bending resistance value, and the bending stiffness value are shown in Table 1.

2.3. Establishment of the Finite Element Model of Beam-Column Joints under Impact Force. The impact force set in the experiment is to apply an impact force along the direction of the steel column at the top of the steel column model and gradually increases the impact force value until the test joint is damaged. The force distribution, local

Table 1: Various properties of steel.

Parameter type	CFST column	Steel pipe column	CFST beam	Steel beam
String bearing load pressure value (KN)	357.0	369.9	—	—
Cross-section bending stiffness value (N•mm^2)	1.99×10^{13}	2.49×10^{13}	—	—
Bending resistance value (kN•m)	—	—	129	121.0
Resistance to bending stiffness value (N•mm^2)	—	—	6.89×10^{12}	6.66×10^{12}

deformation, and the impact load limit are analyzed through the simulation results. Each element to be analyzed is set with a corresponding duration predetermined, and each simulation experiment is set to automatically repeat and stack 1000 instructions [11]. The error range of each superposition is strictly controlled to ensure that the system will not be interrupted during the simulation. If interrupted, the system defaults to the end of the trial and the simulation fails or to success if looping normally. The schematic diagram of the direction in which the impact force is applied is shown in Figure 4.

In the experiment, it should be noted that in addition to the impact force we set in the actual building, there will also be three adhesion forces on the contact surface between the steel pipe and the concrete that need to be considered. These three forces must be damaged before the entire specimen can be completely damaged [12]. The first is the adhesive force between the steel pipe wall and the gel material produced by mixing the cement powder with water, and the second is the occlusal force between the rough protrusions and depressions on the steel pipe wall and the concrete [13]; the third is that there is a friction coefficient between the steel pipe wall and the concrete, so there will be friction. Then, under the action of the impact force, it is not damaged at the same time but has a certain regularity and process in sequence. First, the impact force is small and there is no relative displacement of the joint sliding [14]. Therefore, the friction force and the bite force have no effect for the time being, and the stick force is being pulled. Secondly, after the viscous force reaches the limit, the occlusal part between the pipe wall and the concrete begins to be damaged, resulting in a certain viscous resistance. Then, the impact force continues to increase and the friction force starts when the occlusal surface can no longer keep its relative static until the impact force increases again; the friction force and the part of the occlusal force counteract the impact force.

2.4. Impact Force Parameter Value Setting. In the impact experiment, since it needs to preset a force or equation, a lot of research and sampling are performed before the simulation experiment. The collected data show that the impact force does not grow linearly but is divided into several stages [15]. The first stage is the pulse stage, that is, when it is subjected to the external force, it never touches the contact and the force area increases rapidly. Then, the joint begins to move downward under the impact, the contact surface becomes smaller rapidly, and the impact force also decreases rapidly, resulting in a high-intensity fluctuation. The second stage is platform Section 1. When the impact object touches the joint for the second time, it starts to contact with the joint specimen

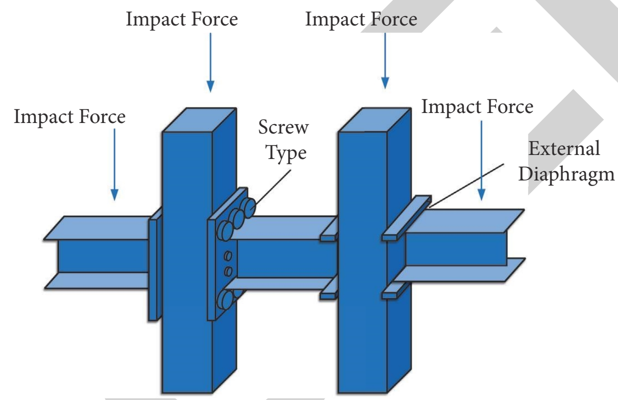

Figure 4: Schematic diagram of the direction of the impact force.

and falls together and then passes through the first stage of a small amplitude and contacts and falls at the same time. Such a reciprocating process forms a relatively stable and gentle impact force. The third stage is the subpulse stage, and when the impact force reaches a certain limit, the specimen and alluvium begin to have tendency to rebound upward because this will slow down the return speed of all flexible joints. Because the impactor's velocity is faster than the element's lower velocity, reducing the recovery speed of each component, this section has reduced its impact. The fourth stage is the platform segment 2. At this time, the impact force is not reduced to zero, the impact object and the joint are relatively static and vibrate with a small amplitude, and the impact force is relatively stable [16]. The size is similar to the second stage.

From the above four-stage force conditions of the actual building impacted, it can simulate an experimental parameter curve. The sampling curve and the simulation curve are shown in Figure 5.

Figure 5(a) is the sampled data, and Figure 5(b) is the simulation curve. The whole simulation curve is a nonlinear curve [17], but it is subdivided into four stages to see that each stage is a linear element. The value corresponding to 4.5 t is set as the limit value of the impact force in the first stage, and the value corresponding to 8.5 t is set as the limit value in the third stage. The action time of the first stage is set to 4 t–5 t, the action time of the second stage is set to 5 t–8 t, the action time of the third stage is set to 8 t–9 t, and the action time of the fourth stage is set to 9 t–12 t.

3. Experimental Results and Analysis

3.1. Analysis on the Limit of the Impact Force of Beam-Column Joints. A unidirectional downward impact force is applied on the top of the column, and the simulation results of the impact bearing limit of the steel beam joint are shown in Figure 6.

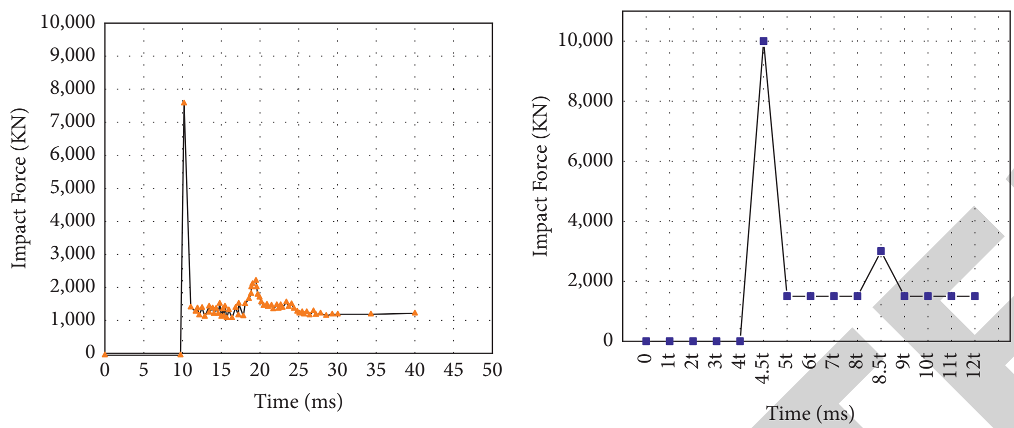

(a) (b)

Figure 5: Impact force curve: (a) experimental parameter curve; (b) sampling curve and simulation curve.

The joint bearing capacity image studies the two connection methods separately, namely, the bolt-type and the external diaphragm-type. Figure 6(a) is the bolt-type, and Figure 6(b) is the external diaphragm-type. Corresponding to the three combinations of specimens, the images can be clearer and easier for us to analyze and compare. The general law can be seen from the image, that is, in the initial stage of impact force application, which is the pulse stage, and the force on the joint presents a linear progressive trend. When the impact force is in platform 1, 2, and subpulse stages, the joint force tends to be gentle and stable. After analysis, the following conclusions can be drawn. For bolt-type joints, the combination of CFST columns and steel beams has a higher impact bearing capacity; for external diaphragm-type joints, the combination of CFST columns and steel beams has a higher impact bearing capacity. Finally, the two methods are compared and found that their impact bearing capacity is almost similar.

A unidirectional downward impact force is applied to the steel beam, and the simulation results of the limit bearing capacity of the steel beam joint are shown in Figure 7.

Figure 7(a) is the bolt-type, and Figure 7(b) is the external diaphragm-type. The general law can be seen from the image, that is, in the initial stage of impact force application, which is the pulse stage, and the force on the joint presents a linear progressive trend. When the impact force is in platform 1, 2, and subpulse stages, the joint force tends to be gentle and stable. After analysis, the following conclusions can be drawn. For bolt-type joints, the combination of CFST columns and steel beams has a higher impact bearing capacity; for external diaphragm-type joints, the combination of CFST columns and steel beams has a higher impact bearing capacity. Finally, it is found by comparing the two methods that the combination of bolt-type CFST columns and steel beams has a higher impact bearing capacity.

3.2. Skeleton Displacement Analysis of Beam-Column Joints under Impact. When the impact force is cyclically superimposed to increase the peak value of the pulse phase, the magnitude of the joint displacement indicates the bearing degree of the joint specimen for the impact force. The simulation results of the ultimate bearing capacity of the steel beam joint are shown in Figure 8.

The displacement curve can represent the relationship between the applied impact force and the joint damage displacement. When the impact force is cyclically superimposed to increase the peak value of the pulse phase, the magnitude of the joint displacement indicates the bearing degree of the joint specimen for the impact force. Figure 8(a) is the bolt-type, and Figure 8(b) is the external diaphragm-type. After analysis, the following conclusions can be drawn. For bolt-type joints, the combination of CFST columns and steel beams has a higher impact bearing capacity; for external diaphragm-type joints, the combination of CFST columns and steel beams has a higher impact bearing capacity. Finally, it is found by comparing the two methods that the combination of bolt-type CFST columns and steel beams has a higher impact bearing capacity.

3.3. Displacement Ductility Analysis of Beam-Column Joints under Impact. For the joints connected by the external diaphragm-type, the measured displacement ductility of each combination is shown in Figure 9.

As shown in the figure, the ductility coefficients of the six models tested are all greater than 2, so they all meet the requirements of the steel structure and the difference is not large. After analysis, the following conclusions can be drawn. For bolt-type joints, the combination of concrete-filled steel tubular columns and steel-beam concrete has better displacement ductility; for external diaphragm-type joints, the combination of CFST columns and steel beams has better displacement ductility. Finally, comparison of the two methods reveals that the combination of the bolt-type CFST column and the steel-beam concrete has better displacement ductility.

3.4. The Bending Stiffness and Strength Degradation of Steel Beam-Column Joints. Under the action of the impact force, the performance degradation of the joint specimen is

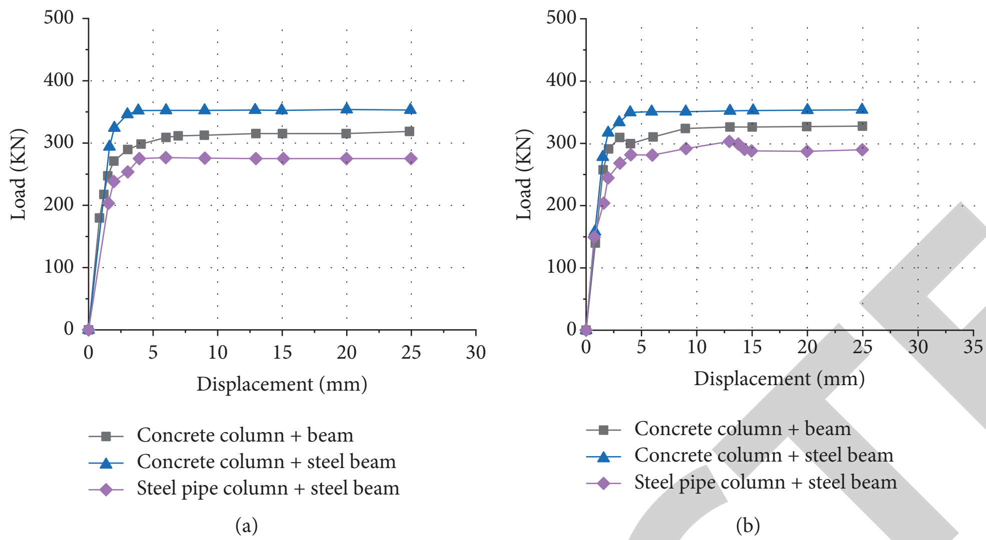

FIGURE 6: Impact curve: (a) bolt-type combination; (b) external diaphragm-type combination.

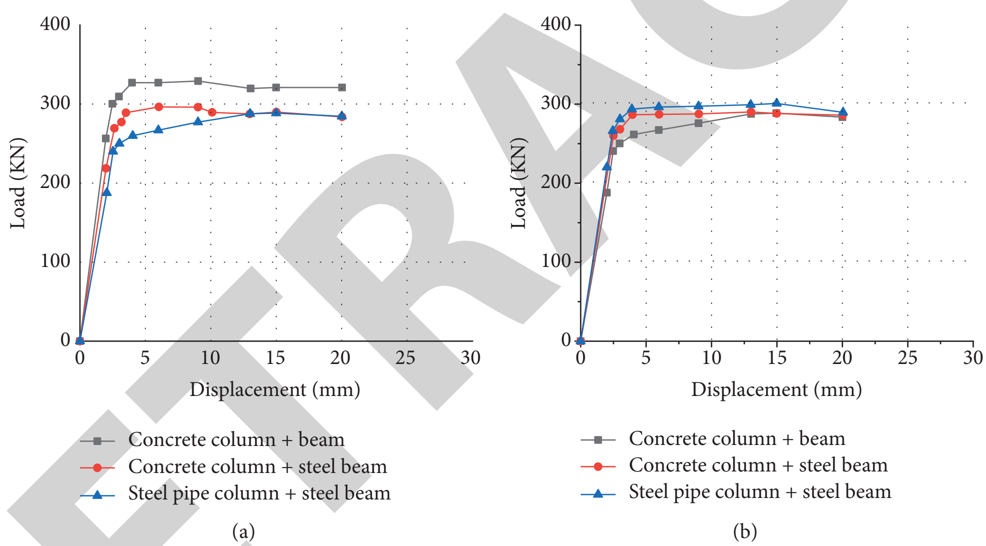

FIGURE 7: Simulation results of the ultimate bearing capacity of the steel beam joint: (a) bolt-type combination; (b) external diaphragm-type combination.

manifested in the degradation of the bending stiffness and bending strength. The degradation of the bending stiffness and bending strength is shown in Figure 10.

Under the action of the impact force, the performance degradation of the joint specimen is manifested in the degradation of the bending stiffness and bending strength. Figures 10(a) and 10(c) are the bolt-type, Figures 10(b) and 10(d) are the external diaphragm-type, Figures 10(a) and 10(b) are bending stiffness data, and Figures 10(c) and 10(d) are flexural strength data. The decrease in bending stiffness means that the joint's resistance to deformation is weakened when it resists the impact force, and the decrease in the bending strength means that the joint's bearing capacity when resisting the impact force is weakened. The overall analysis rule shows that both the bending stiffness and the bending strength decrease significantly after the impact force pulse stage. However, when the impact force enters platform 1, 2, and subimpulse stages, the bending stiffness and strength decrease are more obvious. After analysis, the following conclusions can be drawn. For bolt-type joints, the combination of CFST columns and steel beams decreases slowly and the flexural strength decreases at a moderate rate; for joints connected by the external diaphragm-type, the combination of CFST columns and steel beams decreases slowly in the bending stiffness and the flexural strength. Finally, comparison of these two methods suggests that the combination of CFST columns and steel beams connected by external diaphragms has a slower decline in the bending stiffness and a slower decline in the flexural strength, so it is better.

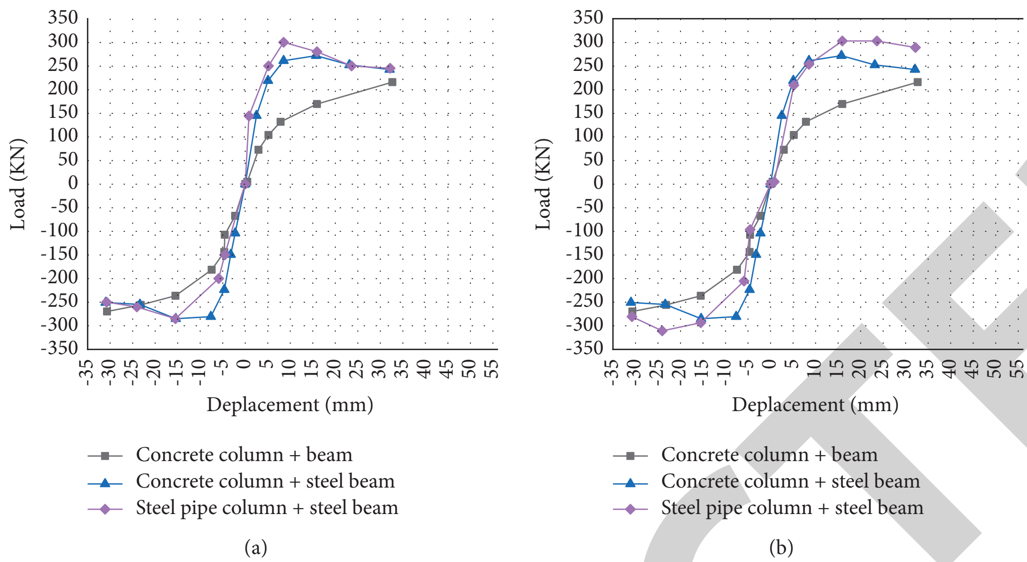

FIGURE 8: Simulation results of the ultimate bearing capacity of the steel beam joint: (a) bolt-type combination; (b) external diaphragm-type combination).

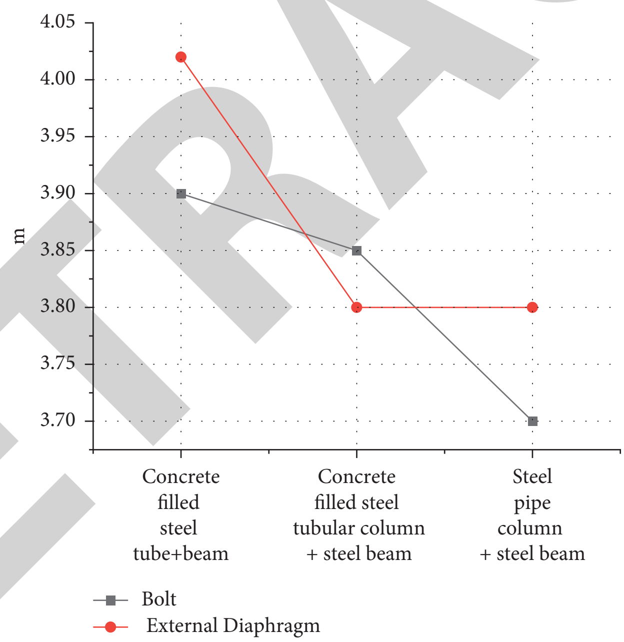

FIGURE 9: Displacement ductility data diagram of each specimen.

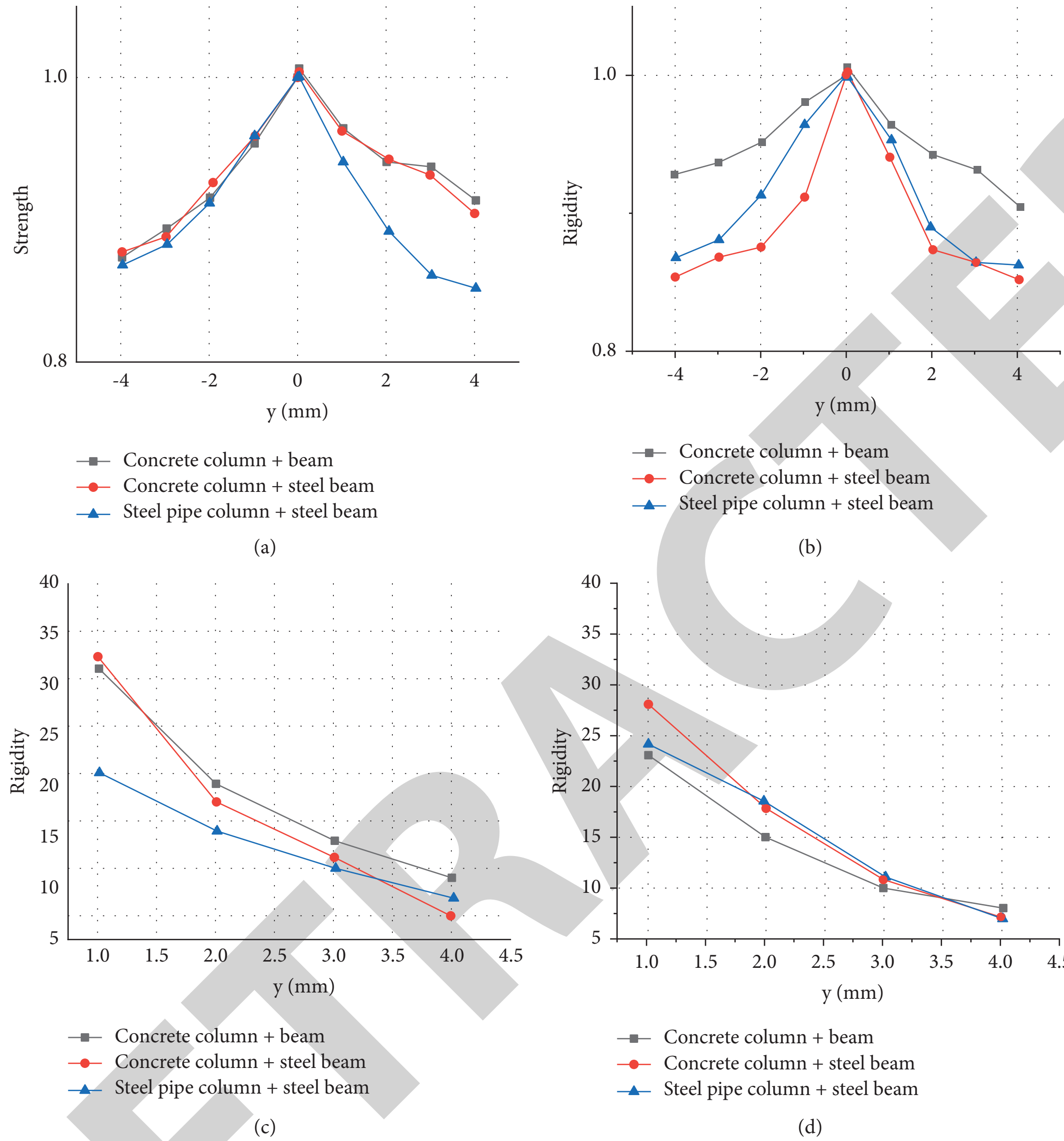

Figure 10: Bending stiffness and strength degradation curves: (a) bolt-type bending stiffness; (b) external diaphragm-type bending stiffness; (c) bolt-type bending stiffness; (d) external diaphragm-type bending stiffness).

4. Conclusion

It is no surprise that high-rise buildings have appeared in cities in recent years, and even low-rise buildings in developed cities are rare, so whether higher spans can still maintain stability and safety will be the biggest problem facing high-rise buildings. Many researchers have performed in-depth research in construction-related fields. Against the background of steel as the core of the basic quality of construction, seismic resistance has become the focus of extensive attention. The concrete analysis and description of the seismic performance is the bending resistance, the degree of deformation and displacement of the steel structure when resisting the impact force, and the degree of bearing capacity for the impact external force. In this work, the most commonly used steel beam and the steel column joint are used as the research object and the applied data of the general impact force are sampled in the actual building to establish a simulated impact force and a finite element model of force. The changes in the performance of the joint under the action of the impact external force are deeply studied through simulation, and finally, the accuracy of the model is confirmed by the calculation. The experimental results comprehensively show that although the transmission mechanisms of the impact force of the six joints are different. Comprehensive analysis of the joint bending stiffness, strength, degree of deformation and displacement, and degree of bearing for impact external force is obtained through calculation and comparison, and a relatively complete conclusion is obtained. It means that the combined joint of the steel tube column concrete and the steel-beam concrete of the bolt-type and the external diaphragm-type has better seismic resistance than the other five joints. Compared with the two, the bolt-type does not need to be welded on the construction site but only needs to be assembled, which can reduce the technical requirements for construction workers, so it is more practical and applicable. Therefore, the research results will be of great significance.

Data Availability

The data used to support the findings of this study are available from the corresponding author upon request.

Conflicts of Interest

The author declares that there are no conflicts of interest.

References

[1] N. Zhandong, "Research on seismic behavior of beam-column joints of new prefabricated steel structure," *IOP Conference Series: Earth and Environmental Science*, vol. 560, no. 1, Article ID 12010, 2020.

[2] Y. Leng, Q. Xu, K. A. Harries, L. Chen, K. Liu, and X. Chen, "Experimental study on mechanical properties of laminated bamboo beam-to-column connections," *Engineering Structures*, vol. 210, no. 5, Article ID 110305, 2020.

[3] C. Wu, S. Yu, J. Liu, and G. Chen, "Development and testing of hybrid precast steel-reinforced concrete column-to- H shape steel beam connections under cyclic loading," *Engineering Structures*, vol. 211, no. 1, Article ID 110460, 2020.

[4] X. Li, Q. Wang, and G. Ma, "Mechanical properties of a novel plastic hinge seismic fuse based on frictional energy dissipation to avoid brittle failures in beamto column moment resistant joints," *Arabian Journal for Science and Engineering*, vol. 45, no. 5, pp. 3695–3706, 2020.

[5] Z. Wang, J. Xu, X. Meng, Z. Huang, and W. Xia, "Study on tensile mechanical properties of polymer cement composite joint sealant under negative temperature," *IOP Conference Series: Earth and Environmental Science*, vol. 676, no. 1, Article ID 012078, 2021.

[6] Z. Wu, Q. Liu, K. Zhu et al., "Cigarette smoke induces the pyroptosis of urothelial cells through ROS/NLRP3/caspase-1 signaling pathway," *Neurourology and Urodynamics*, vol. 39, no. 2, pp. 613–624, 2020.

[7] G. Wang, Y. Luo, X. Li, T. Liu, M. Xu, and D. Qu, "Study on dynamic mechanical properties and meso-deterioration mechanism of sandstone under cyclic impact load," *Arabian Journal for Science and Engineering*, vol. 45, no. 5, pp. 3863–3875, 2020.

[8] C. Jia, Q. Zhang, M. Lei, J. Yu, R. Wang, and J. Liu, "Study on the mechanical properties of outwash deposits with random structure method," *Transportation Safety and Environment*, vol. 3, pp. 3–5, 2021.

[9] F. Xie, W. Liu, B. Gu, and H. Qian, "Study on the component-based model of an all-welded beam-column connection for progressive collapse analysis," *Advances in Civil Engineering*, vol. 2020, Article ID 8847866, 11 pages, 2020.

[10] B. K. Cirpici, "Design analysis of a steel industrial building with wide openings exposed to fire," *Challenge Journal of Structural Mechanics*, vol. 6, no. 3, p. 99, 2020.

[11] X. Xu, L. Li, and A. Sharma, "Controlling messy errors in virtual reconstruction of random sports image capture points for complex systems," *International Journal of System Assurance Engineering and Management*, vol. 4, no. 3, 2021.

[12] S. Shriram, B. Nagaraj, S. Shankar, P. Ajay, and P. Ajay, "Deep learning-based real-time AI virtual mouse system using computer vision to avoid COVID-19 spread," *Journal of Healthcare Engineering*, vol. 2021, Article ID 8133076, 8 pages, 2021.

[13] X. Liu, J. Liu, J. Chen, and F. Zhong, "Degradation of benzene, toluene, and xylene with high gaseous hourly space velocity by double dielectric barrier discharge combined with Mn_3O_4/activated carbon fibers," *Journal of Physics D: Applied Physics*, vol. 55, no. 12, Article ID 125206, 2022.

[14] A. Doomra, S. S. Sandhu, and B. Singh, "Effect of post weld heat treatment on metallurgical and mechanical properties of electron beam welded AISI 409 ferritic steel," *Metallurgical and Materials Engineering*, vol. 26, no. 3, pp. 279–292, 2020.

[15] R. Huang, P. Yan, and X. Yang, "Knowledge map visualization of technology hotspots and development trends in China's textile manufacturing industry," *IET Collaborative Intelligent Manufacturing*, vol. 3, no. 3, pp. 243–251, 2021.

[16] J. Y. Gao, X. Nie, R. Ding, and J. S. Fan, "Experimental study on seismic performance of a new transfer joint in the steel-concrete vertical hybrid structure," *Journal of Constructional Steel Research*, vol. 174, no. 2, Article ID 106259, 2020.

[17] T. Imada and K. Yamagishi, "Analytical study of slide effect of loading object in warehouse building with RC column-steel beam structure," *Journal of Japan Association for Earthquake Engineering*, vol. 20, no. 4, pp. 4–4, 2020.